Combining aerial LiDAR and multi-spectral imagery to assess post-fire regeneration types in a Mediterranean forest

Santiago Martín-Alcón[a,*], Lluís Coll[a,b], Miquel De Cáceres[a,b], Lídia Guitart[a], Mariló Cabré[c], Ariadna Just[c], Jose Ramón González-Olabarría[a]

[a]*Forest Sciences Center of Catalonia (CEMFOR-CTFC), Solsona 25280 Spain*

[b]*CREAF, Cerdanyola del Vallès 08193, Spain*

[c]*Institut Cartogràfic i Geològic de Catalunya (ICGC), Barcelona 08038 Spain*

**Corresponding author, E-mail address: santiago.martin@ctfc.es, Tel.: +34 973 48 17 52*

Abstract

Wildfires play a major role in driving vegetation changes and can cause important environmental and economic losses in Mediterranean forests, especially where the dominant species lacks efficient post-fire regeneration mechanisms. In these areas, post-disturbance vegetation management strategies need to be based on detailed and spatially continuous inventories of the burned area. Here we present a methodology in which we combine airborne LiDAR and multi-spectral imagery for assessing post-fire regeneration types in a spatially continuous way, using a black pine forest burned in 1998 as a case study. Five post-fire regeneration types were obtained by clustering field plot data using Ward's method. Two of the five regeneration types showed high cover of tree species—one clearly dominated by hardwoods, and the other dominated by pines—; a third one presented low to moderate tree cover, being dominated by hardwoods; and the remaining two types matched to areas dominated by soil/herbaceous or shrub layers with very low or no tree-species regeneration. These five classes were used to conduct a supervised classification of remote sensing data using a nonparametric supervised classification technique. Compared against independent field validation points, the remote sensing-based assessment method gave a global classification accuracy of 82.7%. Proportions of regeneration types in the study area indicated a general shift from the former pine-dominated forest toward hardwoods dominance, and showed no serious problems of regeneration failure. Our methodological approach appears appropriate for informing post-disturbance vegetation management strategies over large areas.

Keywords

Post-fire regeneration types, Remote sensing data, Wildfire effects, Post-disturbance management, *Pinus nigra*.

Introduction

Wildfires have been the most important natural disturbance in Mediterranean ecosystems since at least the late Quaternary (Carrión et al. 2010; Pausas et al. 2008). In the Mediterranean region, humans have lived with fire and used it in their agricultural and rural activities during millennia. However, in the last mid century an increase of ignition sources has taken place, causing increasing fire risk and frequency of uncontrolled fires (Gonzalez-Olabarria and Pukkala 2007; San-Miguel-Ayanz et al. 2013; Schelhaas et al. 2003). This increment has been attributed to a combination of factors related, among others, to land abandonment, the increase in the number of days with extreme-fire-hazard weather, and the increasing number of human-related ignition sources (Loepfe et al. 2010). In the Iberian Peninsula, large wildfires (>500 ha) have hit almost every type of forest ecosystem over the last decades, representing almost half of the total burnt area during this period (Cubo María et al. 2012). This scenario of increased fire impacts may be further magnified in the future, as climate forecasts point to prolongation of droughts and hot spells likely to further aggravate forest fire risk (Keenan et al. 2011; Lindner et al. 2010; Piñol et al. 1998; Resco de Dios et al. 2006).

In addition to changes in fire frequency and extent, some areas have suffered an increase in the occurrence of high-intensity crown fires affecting forest types that had not historically been subject to them, such as the montane (sub-Mediterranean) forests dominated by Mediterranean black pine (*Pinus nigra* Arn ssp. *salzmannii)* or *Scots pine (Pinus sylvestris* L.) (Ordoñez and Retana 2004; Pausas et al. 2008; Vilà-Cabrera et al. 2012). These pine species lack direct post-fire regeneration mechanisms and usually show almost nil regeneration after crown fires (Pausas et al. 2008). In these areas substitution of the pines by resprouting hardwoods (mostly *Quercus* species) are generally observed when the latter were present in the understory of the burnt stands (Puerta-Piñero et al. 2011; Rodrigo et al. 2004). In the particular case of *P. nigra* forests, the thick bark and high self-pruning ability of this species allow the persistence of some surviving trees in the form of small islands interspersed across the burned landscape (Ordoñez et al., 2005). The existence of such islands, together with the moderate shade-tolerant character of this species (Niinemets and Valladares, 2006), may lead to greater

64 opportunities for its mid- to long-term colonization of the burned area. In contrast, in the areas
65 without presence of sprouting species or remaining trees, important problems of soil recovery
66 by woody vegetation are likely to arise, leading to increasing soil erosion and forest
67 degradation, and causing long-term environmental and economic damage (Selkimäki et al.
68 2012).

69 Several factors inherent to forests in the Mediterranean basin, such as the small size of
70 forest ownership, slow growth rate due to limited water availability, or the dominance of
71 mountainous terrain, raise the cost of forestry operations and hamper the development of
72 management actions (EFI 2010; Gonzalez-Olabarria et al. 2008), including post-fire restoration
73 measures (Espelta et al. 2003a). These impediments may be in part tempered if detailed and
74 spatially continuous assessments directed to classify the burned area by regeneration success,
75 vegetation types and/or management are available (Vallejo et al. 2012). However, the extent of
76 these types of disturbances makes these detailed and spatially continuous assessments often
77 unattainable through field data gathering. Thus, the general approach used to run post-fire
78 assessments usually involves implementing a statistical sampling design to decide the location
79 of inventory plots (Pausas et al. 2004; Proença et al. 2010; Puerta-Piñero et al. 2012; Shatford et
80 al. 2007) and then applying modeling (i.e. extrapolation) techniques. The use of remote sensing
81 (RS) data has recently emerged as an efficient alternative to provide adequate regeneration
82 assessments over large areas affected by forest disturbances. In this line, some recent studies
83 have used indicators like the Normalized Difference Vegetation Index (NDVI) (Tucker 1979)
84 extracted from satellite imagery to evaluate short-term regeneration success and recovery rates
85 in terms of the total plant cover (Belda and Meliá 2000; Diaz-Delgado et al. 2003; Gouveia et
86 al. 2010; Leeuwen et al. 2010; Viedma et al. 1997; Vila and Barbosa 2010) and even
87 distinguishing the cover of woody shrubs or tree-species regeneration (Riaño et al. 2002;
88 Vicente-Serrano et al. 2011).

89 From an operational point of view, the value of these post-disturbance regeneration
90 assessments might significantly increase if complemented with data describing the structure of
91 the vegetation (e.g. relative cover of the different strata or functional groups, etc.). In relation to

this, Light Detection And Ranging (LiDAR) has recently emerged as a powerful tool for characterizing such structural attributes (Lefsky et al. 2002; Wulder et al. 2012) and it holds great potential for evaluating medium- to long-term post-disturbance regeneration (Debouk et al. 2013; Johnstone et al. 2004). Combining LiDAR data with multi-spectral images could further improve the assessment of post-fire vegetation by making it possible to accurately characterize low vegetation attributes (Erdody and Moskal 2010; Riaño et al. 2007) and to identify individual tree species (Hill et al. 2010; Holmgren et al. 2008; Waser et al. 2011). It also enables to identify vegetation typologies (Bork and Su 2007; Goetz et al. 2010; Mutlu et al. 2008), which may be especially appropriate in the case of low resolution data. Typological characterization of forest stands for management purposes have been widely used on adult forest stands (e.g. Aubury et al. 1990; Herbert and Rebeirot 1985; Martin-Alcon et al. 2012; Reque and Bravo 2008), providing detailed and objective classifications of the stands according to their structural and floristic attributes. In the case of regenerating forest stands, such attributes are expected to largely influence the long-term dynamics of the forest and its accompanying ecosystem services (Elmqvist et al. 2003).

The aim of this study was to develop and test a simple and cost-effective methodology for conducting a detailed and spatially continuous characterization of post-fire regeneration (i.e. recovery of vegetation cover) from widely available remote sensing data, using a large forest fire in the Mediterranean basin as study case. To this purpose, we defined and mapped the main post-fire regeneration types in the study area using a combination of low-resolution airborne LiDAR data (useful for characterizing the three-dimensional structure of plant canopies) with NDVI data computed from multi-spectral data from aerial images, potentially suitable for differentiating between species groups with different spectral signatures. We applied this methodology to the particular case of a large wildfire in a Mediterranean zone, but we anticipate that it should be easily adapted to assess vegetation responses to other forest disturbances and a wide range of forest ecosystems, such as large-scale disease outbreaks or windthrow events.

Material and methods

The methodological approach adopted to assess post-fire regeneration types based on remote sensing data can be summarized in the following steps: (1) remote sensing data processing (raw LiDAR data and raw imagery data), (2) establishment and measurement of a set of field inventory plots located in two subsets of the study area (training areas), (3) selection of the most informative remote sensing (RS) variables to be used as candidate predictors, (4) definition of alternative post-fire regeneration typologies based on training field data, (5) selection of a regeneration typology, on the basis of the classification accuracy of a supervised classification model using RS variables, (6) extrapolation of the regeneration typologies to the whole study area through the application of the corresponding supervised classification model, and (7) validation of the resulting classification using a set of observation points randomly located across the study area (validation stands) (Figure 1).

#Figure 1#

Study area

The study was conducted in an area affected by a large forest fire in the central region of Catalonia (NE Spain). This wildfire burned nearly 24,000 ha in 1998 (Figure 2), leading to almost complete loss of forest cover (Rodrigo et al. 2004). Prior to the wildfire, the area was composed of the typical Mediterranean mosaic-like landscape, with cultivated lands and scrublands (7,700 and 2,000 ha, respectively) interspersed with forest areas (14,000 ha). According to data in the Forest Ecological Inventory of Catalonia (Burriel et al. 2004), the dominant species before the wildfire was black pine (*Pinus nigra* Arn. ssp *salzmanii*), covering 75% of the total forest surface. Aleppo pine (*Pinus halepensis* Mill.) was the second most abundant species, covering 15% of the forest surface. Both black and Aleppo pine forests appeared as pure stands or as two-layered stands, the latter with pine dominating the overstory and resprouting hardwoods the understory (Figure 2). The remaining forest surface was mainly

covered by mixed hardwoods (mainly *Quercus ilex* L. and *Quercus cerrioides* Wilk) and *Pinus sylvestris* L. stands. The area presents a gentle relief with low hills ranging in elevation from 480–910 m.a.s.l. and a dry-sub-humid to sub-humid Mediterranean climate according to the Thornthwaite index.

#Figure 2#

From the total forest area affected by the 1998 wildfire, we selected a portion of 3,973 ha that burned at high severity (i. e. with no remaining adult trees) (Figure 2). Areas affected by roads, agricultural fields and other non-forest uses were excluded from the analysis, leaving a total of 3,192 ha to be used for the post-fire regeneration assessment. Additional criteria to determine the study area were the characteristics of the available remote sensing data, as a minimum seasonal similarity in both LiDAR data and aerial images was required in order to avoid potential mismatches due to the use of data from different seasons (e.g. before and after budbreak in broadleaves). In our particular case, the LiDAR data were taken in the early summer of 2009 and the aerial photographs were taken in the early spring of 2011.

LiDAR data acquisition and processing

LiDAR data were acquired via the LidarCAT project (Cartographic and Geological Institute of Catalonia). The entire study area was covered by seven flight lines captured with an ALS50 II LiDAR sensor mounted on a Cessna Caravan 208B aircraft. The flight date ranged from May 30, 2009 to June 3, 2009. The average first-return point density of these LiDAR data was 0.5 pulses$\cdot$m^{-2} and each pulse captured up to 4 returns. LiDAR point coordinates were adjusted according to the methodology proposed by Kornus and Ruiz (2003). After filtering the clouds, low intensity returns and air points, LiDAR returns were automatically classified with the TerraScan ground classification routine (Terrasolid 2012) in order to differentiate ground from non-ground returns. Ground routine classified ground points by iteratively building a triangulated surface model. The routine started by selecting some local low points that are

172 confident hits on the ground. It was assumed that any 40 by 40 meter area would have at least
173 one hit on the ground and that the lowest point would be a ground hit. The routine built an
174 initial model and started molding the model upwards by iteratively adding new laser points to it.
175 Each added point made the model following the ground surface more closely. Iteration
176 parameters of angle (4º) and distance (1 m) determined how close a point must be to a triangle
177 plane for being accepted as a ground point and added to the model. The remaining non-ground
178 points were visually inspected and manually classified in order to extract wires and towers
179 (since the low point density of the LiDAR data advised against the implementation of automatic
180 algorithms for this purpose). Building roofs were extracted automatically using a new routine
181 which classified non-ground points which formed a planar surface of at least 40 m^2. Finally, the
182 remaining non-ground returns were classified as vegetation, and LiDAR height was replaced by
183 its vertical distance to a triangular irregular network (TIN) generated from ground returns.
184 The LiDAR vegetation point cloud was analyzed in a 10x10 meter regular grid with the
185 FUSION software system (McGaughey and Carson 2003) to obtain structured statistical
186 information on the laser returns. A height of 0.15 meters, predefined from the vegetation field
187 inventory, was used as a threshold to separate woody and shrubby vegetation from herbaceous
188 vegetation and bare soil. Intensity data was normalized by the range normalization to a user-
189 defined standard range (Donoghue et al. 2007; García et al. 2010):

190 $$I' = I \times \frac{R^2}{R_S^2} \quad (1)$$

191 where *I'* is the normalized intensity, *I* is the raw intensity value, *R* is the range (LiDAR sensor-
192 target distance), and R_S is the standard range (in this case 2,225 m, which corresponds to the
193 mean range in the study area). This method eliminated the effect of path length variations on the
194 intensity recorded by the system, providing values equivalent to the intensity that would have
195 been recorded if all points were at the same range. The exact value of the range was not
196 available for each LiDAR point, therefore it was approximated by the use of the difference
197 between the average altitude of the flight and the elevation of each point, and the projected
198 distance between the point and the flight line. This approach should cause smaller errors than

199 the option of using the altitude difference instead of the actual range (Coren and Sterzai 2006;
200 Kukko et al. 2008). Only the first echoes returned from the aboveground vegetation were used
201 for computing a set of LiDAR height and intensity metrics suitable to characterize forest
202 vegetation structure and floristic composition (e.g. Donoghue et al. 2007; García et al. 2010;
203 Holmgren et al. 2008; Latifi et al. 2012; Morsdorf et al. 2006). These metrics were the
204 following: (*i*) percentiles of pulse height (H_P05, H_P10, H_P20, ..., H_P80, H_P90, H_P95)
205 and pulse intensity (Int_P05, Int_P10, Int_P20, ..., Int_P80, Int_P90, Int_P95); (*ii*) the mean
206 (H_MEAN, Int_MEAN), mode (H_MODE, Int_MODE), standard deviation (H_SD, Int_SD),
207 coefficient of variation (H_CV, Int_CV), interquartile range (H_IQ, Int_IQ), skewness (H_Sk,
208 Int_Sk) and kurtosis (H_Kur, Int_Kur) of both pulse height and pulse intensity values. In
209 addition, the following three ratios were generated: percentage of vegetation points (height >
210 0.15 m) in relation to all the first returns (FR_VEG), percentage of vegetation points in relation
211 to all returns (AR_VEG), and percentage of the first returns above the mean height
212 (FR_abMEAN) and the mode (FR_abMODE).

213 *Multi-spectral image acquisition and processing*

214 NDVI imagery were obtained from the Cartographic and Geological Institute of Catalonia
215 annual coverage flights at 22 cm GSD (Ground Sample Distance), and were generated from
216 aerial photos with RGB and near infrared bands. The aerial photos were taken between April 2
217 and April 10 2011, with DMC (Digital Mapping Camera) cameras DMC-26 and DMC-14, and
218 were later ortho-rectified without stitching. The implemented procedure to produce NDVI from
219 DMC imagery used the original DMC LR4 files (low resolution multispectral bands) with
220 absolute radiometric calibration and was based on manufacturer's calibration of the camera,
221 following the methodology proposed by Martínez *et al.* (2012). Radiance values from the red
222 and near infrared bands, and its respective reflectances (i.e. ratio between incoming energy from
223 the sun and reflected energy modulated by some geometric factors such as location, data and
224 time of exposure during acquisition) were obtained for each pixel using the following equations:

$$R = \frac{\pi \times L_R}{\mu \times E_O} \quad (2)$$

$$NIR = \frac{\pi \times L_{NIR}}{\mu \times E_O} \quad (3)$$

where L_R-and L_{NIR} are radiance values from the red and the near infrared bands, μ is a geometric factor and E_0 is the extraterrestrial solar radiance. Then, NDVI was calculated using the following equation:

$$NDVI = \frac{(NIR - R)}{(NIR + R)} \quad (4)$$

where R and NIR correspond to the reflectance values of each pixel from the red and the near infrared band, respectively. NDVI values were then aggregated to match the same 10×10 meter grid as that use to aggregate the LiDAR data and a set of NDVI statistics potentially suitable to describe regeneration structure and composition was calculated. The quartiles of NDVI distribution (NDVI_Q1, NDVI_Q2 and NDVI_Q3), the interquartile range (NDVI_IQ), mean (NDVI_MEAN), coefficient of variation (NDVI_CV), and standard deviation of the NDVI values (NDVI_SD) were obtained. NDVI values in the regenerating area generally ranged between 0 and 0.6. On this basis, the portion of each 10x10 meter cell presenting NDVI values within a variety of sub-ranges were computed, using 0.05 increments (0.15-0.2, …, 0.55-0.6), 0.10 increments (0.15-0.25, ..., 0.45-0.55), and 0.15 increments (0.15-0.3, 0.3-0.45 and 0.45-0.6), in order to maximize the chance of differentiating species or groups of them based on their different NDVI values.

Field data gathering

A field inventory was performed in order to define post-fire regeneration types. The inventory consisted of a set of forty-four 10×10 meter plots placed along two sub-areas considered representative of the overall study area (named training areas) (Figure 2). Stratified random sampling was applied to capture the range of regeneration patterns in the training areas. For this purpose, LiDAR variables which were expected to describe plant height distribution and the distance to unburned patches were used to ensure that we covered both the structural (relative

abundance of trees) and compositional gradients (since pines are expected to be more abundant near the unburned patches) characterizing the post-fire vegetation. For each plot, a set of variables describing the floristic composition and aboveground biomass structure were measured. These were the percentage of the plot area covered by soil or herbs (%SOIL), low shrub species (0.15-0.5 m tall) (%LOW SHRUBS), high shrub species (>0.5 m) (%HIGH SHRUBS), pine regeneration (%PINES) and tree species regeneration (i.e. referred to all trees including pines) (%TREES). Low and high shrub covers were later summed as %SHRUBS. We also measured mean height (cm) of all tree species (HTREES), pines (HPINES) and hardwoods (HHW). To improve the accuracy of the measured vegetation variables each 10×10 meter plot was subdivided into 2.5×2.5 m subplots. The variables were measured at the subplot level and converted into plot level values by averaging the values of the measured sub-plots within each plot.

Remote sensing data reduction

A first pre-selection of the sixty-four initially considered LiDAR- and NDVI-derived metrics was executed in order to avoid using redundant variables as candidate predictors. Principal Component Analysis (PCA) with a Varimax rotation was executed on the whole set of RS data in order to identify groups of highly collinear variables. In parallel, we computed Pearson correlation coefficients to measure the associations between RS variables and the list of forest variables measured in the field plots. A total of fourteen variables from the original sixty-four were finally preselected. These variables were the ones showing the highest correlation with field variables among each group of highly collinear variables (i. e. variables with very similar PCA factor loadings). They comprised five height metrics (coefficient of variation, kurtosis, 10th and 95th percentile height, percentage of first returns of vegetation, and percentage of first returns above the mode of the height distribution), three LiDAR intensity metrics (standard deviation, 50th and 90th percentile intensity), and five NDVI-derived variables (1st quartile NDVI, percentage of plot with NDVI between 0.45-0.5, 0.25-0.35, 0.15-0.3, and 0.45-0.6).

Definition of post-fire regeneration types

A subset of the variables measured in the field (%SOIL, %PINES and %TREES) were deemed sufficient to define post-fire regeneration types, as they described the distribution of the plot cover among the main strata (soil/herbs, trees and, indirectly, shrubs), and the main floristic groups of the tree layer (pines and hardwoods). The forty-four training plots were clustered according to their squared Euclidean distances using Ward's hierarchical method (Ward 1963), based on these variables. Several alternative partitions of the resulting dendrogram (i.e., those exhibiting high between-groups distance (Hair et al. 2009) and strong ecological rationale) were saved.

Development of the classification model

We used pre-selected RS variables from the field plots and the Random Forest classification algorithm (Breiman 2001) to evaluate the different partition alternatives and to obtain a model for the classification of the whole study area. Random Forest (RF) is a nonparametric supervised classification technique that has shown good performance in classifying remotely sensed data (e.g. Falkowski et al. 2009; Hudak et al. 2012). The RF technique uses a bootstrap approach for achieving higher accuracies while simultaneously addressing over-fitting problems associated with traditional classification tree models. A large number of classification trees are produced from a random subset of training data (approximately 63% random subset), permutations are introduced at each node, and the most common classification result is selected. We ran each RF model with 5,000 bootstrap replicates (i.e., individual classification trees). With the aim of avoiding bias in the prediction caused by imbalanced classes, the number plots per class in bootstrap samples was equal to the number of plots of the less frequent class (Evans and Cushman 2009). Out-of-bag (OOB) error estimates were calculated for each tree by classifying the portion of training data not selected in the bootstrap sample, and overall accuracy was calculated by averaging error rates across all trees in the model; this is analogous to cross-validated accuracy estimates (Cutler et al. 2007).

A model selection procedure (i.e., variable reduction) was employed to select the optimal RS variables to use in the classification of post-fire regeneration types. The procedure was formulated to develop the most parsimonious classification model, while retaining the highest possible classification accuracy. We ran a Random Forest model selection function that uses Model Improvement Ratio (MIR) standardized importance values (Evans et al. 2011; Evans and Cushman 2009) to objectively choose the most important RS variables for predicting the regeneration type of each plot. The MIR uses the permuted variable importance, represented by the mean decrease in OOB error, standardized from zero to one. The variables were subset using 0.10 threshold increments on the original model's variable importance, with all variables above the threshold retained for each model. Each subset model was compared and the model that exhibited the lowest total OOB and lowest maximum within-class error was selected. After selecting the best model for each one of the different alternative partitions, we determined the final regeneration typology as that whose classification model had obtained the highest classification accuracy. For this study, the RF algorithm was implemented using the RandomForest package (Liaw and Wiener 2002) in the R statistical program (R Development Core Team 2007).

Mapping of regeneration types and field-based validation

Each 10 x 10 m plot in the study area was classified into one of the regeneration types by applying the final classification model on the RS variables. Regeneration types were then mapped and a set of landscape metrics were generated for explaining the spatial configuration of the landscape according to the distribution of regeneration patches. These size- and shape-related metrics were the area and percentage covered by each regeneration type, the percentage of the type area by patch size classes, the mean patch size (PSm) and its Coefficient of Variation (PScv), and the Mean Shape Index (MSI), as defined by Rempel *et al*. (2012).

The validity of the final classification for the whole study area was evaluated by comparing the regeneration type assignations made from supervised classification of remote-sensing data (using the classification model generated by RF) against visual assessments

329 obtained in the field. For this purpose, 15 sampling points per regeneration type were distributed
330 along the study area using stratified random sampling (Figure 2). An independent user was
331 asked to assign each of these stands to one of the regeneration types, based on a visual
332 examination of the stand characteristics, using the type descriptions in terms of forest variables
333 (see Table 1 and Figure 3) as a guide. Measures of height and cover of the different vegetation
334 strata were taken when visual estimation was not obvious. Finally, a confusion matrix was
335 generated to estimate the accuracy of the remote sensing-based assignations with respect to the
336 visual ones.

337 ## Results

338 *Post-fire regeneration typologies*

339 Dendrogram resulting from the application of Ward's clustering method on the variables
340 measured in the 44 field plots[1] led to three possible choices for the placement of the cut-off
341 point of the hierarchical tree (i.e. three partition alternatives), creating a 4-type, a 5-type and a 6-
342 type partitions. By comparing the classification accuracy of the models developed using
343 Random Forest for the 4, 5, and 6 type partitions, we found the 5-type one to be the best in
344 terms of overall accuracy, with 79.55% of the plots being correctly classified (i.e. OBB estimate
345 of error rate was 20,45%), with the use of 6 RS variables as predictors. The 4-type[2] and 6 –type[3]
346 partitions presented accuracies of 75% and 71,45% respectively, and none of them selected less
347 than 6 RS variables as predictors. Therefore, type-5 partition was selected as the basis for
348 representing the regeneration types (Table 1). The characteristics of the five regeneration types
349 were as follows: the first type was characterized by a very low vegetation cover (TYPE 1); a
350 second type had very low tree regeneration but remarkable shrubs abundance (TYPE 2); the
351 third type included hardwoods in low to moderate cover, mixed with shrubs (TYPE 3); the
352 fourth type presented high cover of hardwoods regeneration (TYPE 4); and the fifth type

[1] Figure 1S in Supplementary material
[2] Table 1S in Supplementary material
[3] Table 2S in Supplementary material

consisted of stands dominated by pine regeneration in moderate to high cover (TYPE 5) (Table 1, Figure 3).

#Table 1#

#Figure 3#

The six RS variables selected to identify the five regeneration types were: the 10th and 95th percentile height (H_P10 and H_P95), the percentage of first returns above the mode of the height distribution (H_abMODE), the coefficient of variation of the height distribution (H_CV), the 1st quartile NDVI (NDVI_Q1) and the percentage of plot with NDVI between 0.15-0.3 (NDVI_15_30) (Figure 4). OOB classification accuracies of the RF model by regeneration type were 80% for TYPE 1, 100% for TYPE 2, 81.8% for TYPE 3, 70% for TYPE 4, and 76.9% for TYPE 5.

#Figure 4#

Mapping post-fire regeneration types and validation with visual estimates

The whole study area (3191.8 ha) was classified into the five regeneration types (Figure 5). More than a decade after the wildfire, almost a half of the area (42.6%) showed high tree cover with clear dominance of resprouting hardwoods (TYPE 4). About 17% of the study area was still dominated by resprouting hardwoods, but with low to moderate tree cover (TYPE 3). Pine regeneration appeared in moderate to high cover in approximately 11% of the study area. Finally, the rest of the area showed sparse or no tree regeneration (TYPE 2 and 1) (Table 2). Patches of TYPE 1 and TYPE 3 were usually very small (i. e. with an area smaller than 0.1 ha), with TYPE 1 showing the most regular patch shape (i. e. closer to a circular shape). In contrast, TYPE 4 was the one presenting the highest area covered by large patches (0.1-1 ha, 1-5 ha and larger than 5 ha) and showed the most irregular shapes. TYPE 2 and TYPE 5 were also present in a wide range of patch sizes, but in them small patches were more common than in TYPE 4.

#Figure 5#

#Table 2#

The evaluation of classification accuracy compared to visual estimation resulted in 82.7% well-classified plots (between 74.1% and 91.2% well classified with a 95% confidence interval), being close to the OOB classification accuracy obtained for the training dataset. TYPEs 1 and 5 showed the highest classification accuracy, at 93.3% (80.7%–100%) for TYPE 1 and approximately 92.3% (77.8%–100%) for TYPE 5. The classification of TYPE 4 was also highly accurate, with 84.6% (65%–100%) of plots appropriately classified. Finally, TYPEs 2 (shrubs dominance with very low tree cover) and 3 (low to moderate tree cover dominated by hardwoods) reported lower classification accuracies, with 72.2% (51.5-92.9%) and 75% (53.8-96.2%) of plots appropriately classified, respectively.

Discussion

This study presents a methodological approach that combines airborne LiDAR data and single-date NDVI data computed from aerial images to provide precise geo-referenced and spatially continuous information on post-fire regeneration over a large area. The presented methodology was not intended for short-term assessments—for which analysis of NDVI values extracted from satellite imagery may be enough (Diaz-Delgado et al. 2003; Gouveia et al. 2010; Leeuwen et al. 2010; Vicente-Serrano et al. 2011; Vila and Barbosa 2010), but for mid-to-long-term assessments which are crucial for appropriately designing and planning post-disturbance silvicultural treatments (Alloza and Vallejo 2006; Bauhus et al. 2013; Stephens et al. 2010). The information generated by this methodology provides forest stand structure and composition information that can be used to predict its potential evolution patterns, detect of areas with persistent regeneration problems, and delimit forest stands for planning management operations. This ultimately enables management interventions to be prioritized and allocated.

There are some differences between our RS-based assessment and evaluations as traditionally made from field-based inventories. On one hand, the level of detail in describing the post-fire vegetation communities is in general higher in field-based inventories where measurements are conducted at individual plant level (e.g. Curt et al. 2009; Proença et al. 2010). However, RS-based assessments entail less time and fewer spatial constraints than field inventories, as they are much less time-consuming and less exposed to the uncertainties associated with inference and estimation from sample surveys in areas showing fine-scale heterogeneity. Assessments based on RS data also allow estimating quantitative tree and forest attributes across large areas by using regression methods (e.g. Andersen et al. 2005; García et al. 2010; Latifi et al. 2012; Wulder et al. 2009). However, that approach requires working with high resolution LiDAR data, especially when forest attributes are related to low vegetation. In our case, we aggregated remote sensing metrics to the plot-level (10x10 meter) to make a community-based assessment instead of a plant-based one, and we estimated forest types instead of quantitative forest attributes, in concordance with the potential and limitations of the available low resolution LiDAR data. Our approach permits discerning between regeneration types by using height and intensity variables from LiDAR data and NDVI metrics computed from single-date multi-spectral aerial imagery, thus providing forest managers with most of the information they need for mid-term operational planning of restoration activities and silvicultural operations (Vallejo et al. 2012). In addition, the provision of continuous spatially-explicit information at the landscape scale allows easy implementation of relevant forestry applications such as the characterization and mapping of forest canopy fuels and fire risk (Erdody and Moskal 2010; García et al. 2011; González-Olabarria et al. 2012; Mutlu et al. 2008; Pierce et al. 2012; Riaño et al. 2007). The resulting maps of regeneration types also offer a starting point for the analysis of post-disturbance vegetation dynamics at large scales (Debouk et al. 2013; Goetz et al. 2010; Holmgren et al. 2008). Our methodology is appropriate for large-scale assessment, since regional and national LiDAR coverages are often collected at low-resolution. The NDVI data we used were derived from 4-band aerial imagery, which are also more and more used for national surveys. They have higher spatial resolution that the ones derived from satellite

436 imagery, although they are more limited for multi-temporal analyses due to the generally low
437 temporal resolution.

438 Our approach requires a prior categorization of the vegetation that is to be extrapolated
439 using RS data. Such characterization can be achieved by generating vegetation typologies from
440 the analysis of quantitative field data (as presented here), but also by using existing
441 classifications when types of vegetation are previously known (Falkowski et al. 2009). Other
442 areas may have different pre-fire forest composition and structure, or be more or less severely
443 impacted by fire, and present different post-fire regeneration trajectories. Thus the number and
444 characteristics of the regeneration types may change from one area to the other, and the RS
445 variables selected for the classification model will be different in each particular case, since
446 other types of vegetation may be better explained by different combination of RS variables. In
447 our case, the best fit was attained just with a combination of LiDAR height and NDVI variables.
448 LiDAR normalized intensity variables were not found to be essential in discerning our
449 regeneration types, but they could be more important in other cases (Bork and Su 2007;
450 Donoghue et al. 2007; García et al. 2010).

451 Our methodology is applicable as long as the input data (LiDAR and NDVI data) is
452 available and the chosen typologies can be accurately reproduced using supervised classification
453 of RS data. Even so, our approach calls for a certain period of time to pass between the
454 occurrence of the disturbance and the acquisition of the RS data to allow height differentiation
455 between species and groups of species, in order to exploit the full potential of combining
456 LiDAR and NDVI data for vegetation characterization. Other aspects which must be considered
457 when applying this methodology are the characteristics of the RS data available, particularly in
458 terms of collection dates (year and season) and spatial resolution. In this regard, increasing
459 intensity of field sampling would be necessary for a disturbed area where date and season of
460 collection of the RS data are not comparable. Meanwhile, the spatial resolution of the RS data
461 available may dictate how the level of detail in characterizing regeneration types needs to be
462 adapted. Finally, the use of this methodology also requires good knowledge of the vegetation in
463 the specific area under study and a decision about the pretended level of detail when

464 categorizing it, in order to adequately design the field inventory, with more heterogeneous
465 environments typically requiring a denser network of field plots.
466 The five regeneration types obtained in our study area adequately represent the wide
467 range of post-fire conditions described in previous field studies (Retana et al. 2012; Retana et al.
468 2002; Rodrigo et al. 2004). Furthermore, the results of the field validation revealed high (>80%)
469 overall classification accuracy levels. For three of five types, the field validation matched the
470 classification implemented through RS variables in over 80% of cases. The TYPEs dominated
471 by shrubs with very low tree cover (i.e. TYPE 2) and by low to moderate tree cover dominated
472 by hardwoods (i.e. TYPE 3) showed sensibly lower accuracy levels (of around 70-75%). Most
473 of the misclassified TYPE 2 plots were assigned to TYPE 3, meaning that the cover of
474 hardwoods was overestimated in the classification model based on RS data. Misclassified TYPE
475 3 plots were assigned to TYPE 4 (very similar to TYPE 3, as they are dominated by hardwoods
476 regeneration, but with higher hardwoods cover). Overall, misclassification problems could be
477 considered relatively small and occurred among closely related regeneration types. Interestingly,
478 two of the regeneration types of major interest for management purposes (TYPEs 1, with
479 defective cover of woody vegetation, and 5, with moderate to high cover of pine regeneration),
480 were identified with high accuracy. In the case of TYPE 5, this may indicate very good
481 performance of NDVI-derived variables for species differentiation, as previously shown in other
482 studies (Hill et al. 2010; Key et al. 2001).
483 Regarding the spatial distribution of the forest regeneration, we found hardwoods
484 resprouts to be presently dominating near 60% of the area formerly dominated by pines. These
485 results demonstrate the important species dominance shifts that crown fires may induce in
486 Mediterranean black pine forests, as reported by Rodrigo et al. (2004). However, it should be
487 stressed that the level of detail achieved in our study did not allow proper identification of the
488 presence of small pines on forest areas dominated by high shrubs or hardwoods, leading to
489 certain underestimation of the pine regeneration. Interestingly, we also found less than 10% of
490 the burned area to be in high risk of soil erosion due to a defective cover of woody vegetation.

491 This lack of regeneration appeared in very small patches, which sometimes could be associated
492 to the presence of small rocky outcrops.

493 The information generated through our methodological approach should be useful for the
494 definition of vegetation management and restoration strategies over large areas affected by
495 disturbances, as it helps to identify areas where woody species are struggling to regenerate (thus
496 potentially needing restoral actions) and to provide information on areas showing regeneration
497 success and their current vegetation structure. For example, restoration actions designed to
498 facilitate tree cover recovery could be envisaged areas of our case study where the predominant
499 post-fire regeneration pattern was identified as TYPE 1 and TYPE 2, especially in the larger
500 patches (more frequently classed as TYPE 2). In parallel, early thinning interventions designed
501 to reduce competition to increase tree growth and vigor and to reduce the amount and continuity
502 of fuels could be planned for patches classified as TYPE 5 (Gonzalez-Olabarria et al. 2008;
503 Moya et al. 2008; Verkaik and Espelta 2006), while coppice thinning could be proposed for
504 stands classified as TYPE 4 (Cotillas et al. 2009; Espelta et al. 2003b; Sanchez-Humanes and
505 Espelta 2011).

506 **Acknowledgements**

507 This research was primarily supported by the Spanish Ministry of Science and Innovation via
508 the RESILFOR project (AGL2012-40039-C02-01). It also was part of a cooperation agreement
509 between the Forest Sciences Center of Catalonia and the Institut Cartogràfic i Geològic de
510 Catalunya aimed at using aerial remote sensing data for forest characterization. The Catalan
511 Agency for Management of University and Research Grants provided S.M.A. with support
512 through a 'pre-doctoral' grant (FI-DGR) and the Spanish Ministry of Science and Innovation
513 provided L.C., JR.G. and M.C. through post-doctoral ‘Ramon y Cajal’ contracts. Finally,
514 authors are very grateful to Vicent Vidal, Sergio Martinez and Assu Gil for their invaluable help
515 in the collection of the field data.

References

Alloza, J.A., and Vallejo, R. 2006. Restoration of burned areas in forest management plans. *In* Desertification in the Mediterranean Region. A Security Issue. *Edited by* W. Kepner and J. Rubio and D. Mouat and F. Pedrazzini. Springer Netherlands. pp. 475-488.

Andersen, H.-E., McGaughey, R.J., and Reutebuch, S.E. 2005. Estimating forest canopy fuel parameters using LIDAR data. Remote Sens. Environ. **94**(4): 441-449. doi: 10.1016/j.rse.2004.10.013.

Aubury, S., Bruciamacchie, M., and Druelle, P. 1990. L'inventaire typologique: Un outil performant pour l'elaboration des amenagements ou plans simples de gestion. Rev. For. Fr.(4): 429-444.

Bauhus, J., Puettmann, K.J., and Kühne, C. 2013. Close-to-nature forest management in Europe. *In* Managing forests as complex adaptive systems: building resilience to the challenge of global change. *Edited by* C. Messier and K.J. Puettmann and K.D. Coates. The earthscan forest library, NY.

Belda, F., and Meliá, J. 2000. Relationships between climatic parameters and forest vegetation: application to burned area in Alicante (Spain). Forest. Ecol. Manag. **135**(1–3): 195-204. doi: 10.1016/S0378-1127(00)00310-8.

Bork, E.W., and Su, J.G. 2007. Integrating LIDAR data and multispectral imagery for enhanced classification of rangeland vegetation: A meta analysis. Remote Sens. Environ. **111**(1): 11-24. doi: 10.1016/j.rse.2007.03.011.

Breiman, L. 2001. Random Forests. Machine Learning **45**(1): 5-32. doi: 10.1023/A:1010933404324.

Burriel, J.A., Gracia, C., Ibàñez, J.J., Mata, T., and Vayreda, J. 2004. Inventari Ecològic i Forestal de Catalunya. CREAF, Bellaterra.

Carrión, J.S., Fernández, S., González-Sampériz, P., Gil-Romera, G., Badal, E., Carrión-Marco, Y., López-Merino, L., López-Sáez, J.A., Fierro, E., and Burjachs, F. 2010. Expected trends and surprises in the Lateglacial and Holocene vegetation history of the Iberian Peninsula and Balearic Islands. Rev. Palaeobot. Palynol. **162**(3): 458-475. doi: 10.1016/j.revpalbo.2009.12.007

Coren, F., and Sterzai, P. 2006. Radiometric correction in laser scanning. Int. J. Remote Sens. **27**(15): 3097-3104. doi: 10.1080/01431160500217277.

Cotillas, M., Sabaté, S., Gracia, C., and Espelta, J.M. 2009. Growth response of mixed mediterranean oak coppices to rainfall reduction. Could selective thinning have any influence on it? Forest. Ecol. Manag. **258**(7): 1677-1683. doi: 10.1016/j.foreco.2009.07.033.

CREAF. 1993. Mapa de cobertes del sòl de Catalunya v1. *Edited by* D.d.A. Centre de Recerca Ecològica i Aplicacions Forestals, Ramaderia, Pesca, Alimentació i Medi Natural, Interior i Territori i Sostenibilitat. Generalitat de Catalunya

Cubo María, J.E., Enríquez Alcalde, E., Gallar Pérez-Pastor, J.J., Jemes Díaz, V., López García, M., Mateo Díez, M.L., Muñoz Correal, A., and Parra Orgaz, P.J. 2012. Los incendios forestales en España. Decenio 2001-2010.

Curt, T., Adra, W., and Borgniet, L. 2009. Fire-driven oak regeneration in French Mediterranean ecosystems. Forest. Ecol. Manag. **258**(9): 2127-2135. doi: 10.1016/j.foreco.2009.08.010.

Cutler, D.R., Edwards, T.C., Beard, K.H., Cutler, A., Hess, K.T., Gibson, J., and Lawler, J.J. 2007. Random Forests for classification in ecology. Ecology **88**(11): 2783-2792. doi: 10.1890/07-0539.1.

Debouk, H., Riera-Tatché, R., and Vega-García, C. 2013. Assessing Post-Fire Regeneration in a Mediterranean Mixed Forest Using Lidar Data and Artificial Neural Networks. Photogramm. Eng. Remote Sens. **79**(12): 1121-1130. doi: 10.14358/PERS.79.12.1121.

DGCN. 2001. Mapa Forestal de España. Escala 1:50.000. Cataluña. Organismo Autónomo de Parques Nacionales (MMA), Madrid.

Diaz-Delgado, R., Llorett, F., and Pons, X. 2003. Influence of fire severity on plant regeneration by means of remote sensing imagery. Int. J. Remote Sens. **24**(8): 1751-1763. doi: 10.1080/01431160210144732.

Donoghue, D.N.M., Watt, P.J., Cox, N.J., and Wilson, J. 2007. Remote sensing of species mixtures in conifer plantations using LiDAR height and intensity data. Remote Sens. Environ. **110**(4): 509-522. doi: 10.1016/j.rse.2007.02.032.

EFI. 2010. A Mediterranean Forest Research Agenda. MFRA. European Forest Institute.

Elmqvist, T., Folke, C., Nystrom, M., Peterson, G., Bengtsson, J., Walker, B., and Norberg, J. 2003. Response diversity, ecosystem change, and resilience. Front. Ecol. Environ. **1**(9): 488-494. http://dx.doi.org/10.1890/1540-9295(2003)001[0488:RDECAR]2.0.CO;2

Erdody, T.L., and Moskal, L.M. 2010. Fusion of LiDAR and imagery for estimating forest canopy fuels. Remote Sens. Environ. **114**(4): 725-737. doi: 10.1016/j.rse.2009.11.002.

Espelta, J.M., Retana, J., and Habrouk, A. 2003a. An economic and ecological multi-criteria evaluation of reforestation methods to recover burned Pinus nigra forests in NE Spain. Forest. Ecol. Manag. **180**(1-3): 185-198. doi: 10.1016/s0378-1127(02)00599-6.

Espelta, J.M., Retana, J., and Habrouk, A. 2003b. Resprouting patterns after fire and response to stool cleaning of two coexisting Mediterranean oaks with contrasting leaf habits on two different sites. Forest. Ecol. Manag. **179**(1-3): 401-414. doi: 10.1016/s0378-1127(02)00541-8.

Evans, J., Murphy, M., Holden, Z., and Cushman, S. 2011. Modeling Species Distribution and Change Using Random Forest. *In* Predictive Species and Habitat Modeling in Landscape Ecology. *Edited by* C.A. Drew and Y.F. Wiersma and F. Huettmann. Springer New York. pp. 139-159.

Evans, J.S., and Cushman, S.A. 2009. Gradient modeling of conifer species using random forests. Landsc. Ecol. **24**(5): 673-683. doi: 10.1007/s10980-009-9341-0.

Falkowski, M.J., Evans, J.S., Martinuzzi, S., Gessler, P.E., and Hudak, A.T. 2009. Characterizing forest succession with lidar data: An evaluation for the Inland Northwest, USA. Remote Sens. Environ. **113**(5): 946-956. doi: 10.1016/j.rse.2009.01.003.

García, M., Riaño, D., Chuvieco, E., and Danson, F.M. 2010. Estimating biomass carbon stocks for a Mediterranean forest in central Spain using LiDAR height and intensity data. Remote Sens. Environ. **114**(4): 816-830. doi: 10.1016/j.rse.2009.11.021.

García, M., Riaño, D., Chuvieco, E., Salas, J., and Danson, F.M. 2011. Multispectral and LiDAR data fusion for fuel type mapping using Support Vector Machine and decision rules. Remote Sens. Environ. **115**(6): 1369-1379. doi: 10.1016/j.rse.2011.01.017.

Goetz, S.J., Sun, M., Baccini, A., and Beck, P.S.A. 2010. Synergistic use of spaceborne lidar and optical imagery for assessing forest disturbance: An Alaska case study. J. Geophys. Res.-Biogeo. **115**(G2): G00E07. doi: 10.1029/2008JG000898.

González-Olabarria, J.-R., Rodríguez, F., Fernández-Landa, A., and Mola-Yudego, B. 2012. Mapping fire risk in the Model Forest of Urbión (Spain) based on airborne LiDAR measurements. Forest. Ecol. Manag. **282**: 149-156. doi: 10.1016/j.foreco.2012.06.056.

Gonzalez-Olabarria, J.R., Palahi, M., Pukkala, T., and Trasobares, A. 2008. Optimising the management of Pinus nigra Arn. stands under endogenous risk of fire in Catalonia. Inv. Agrar: Sist. Recursos Fores. **17**(1): 10-17.

Gonzalez-Olabarria, J.R., and Pukkala, T. 2007. Characterization of forest fires in Catalonia (north-east Spain). Eur. J. For. Res. **126**(3): 421-429. doi: 10.1007/s10342-006-0164-0.

Gouveia, C., DaCamara, C.C., and Trigo, R.M. 2010. Post-fire vegetation recovery in Portugal based on spot/vegetation data. Nat. Hazard. Earth Sys. **10**(4): 673-684.

Hair, J.F., Tatham, R.L., Anderson, R.E., and Black, W. 2009. Multivariate Data Analysis. 7th ed. Pearson. pp. 751.

Herbert, I., and Rebeirot, F. 1985. Les futaies jardinées du Haut-Jura. Rev. For. Fr. **XXXVII**(6): 465-481.

Hill, R.A., Wilson, A.K., George, M., and Hinsley, S.A. 2010. Mapping tree species in temperate deciduous woodland using time-series multi-spectral data. Appl. Veg. Sci. **13**(1): 86-99. doi: 10.1111/j.1654-109X.2009.01053.x.

Holmgren, J., Persson, Å., and Söderman, U. 2008. Species identification of individual trees by combining high resolution LiDAR data with multi-spectral images. Int. J. Remote Sens. **29**(5): 1537-1552. doi: 10.1080/01431160701736471.

Hudak, A.T., Strand, E.K., Vierling, L.A., Byrne, J.C., Eitel, J.U.H., Martinuzzi, S., and Falkowski, M.J. 2012. Quantifying aboveground forest carbon pools and fluxes from repeat LiDAR surveys. Remote Sens. Environ. **123**: 25-40. doi: 10.1016/j.rse.2012.02.023.

Johnstone, J.F., Chapin Iii, F.S., Foote, J., Kemmett, S., Price, K., and Viereck, L. 2004. Decadal observations of tree regeneration following fire in boreal forests. Can. J. For. Res. **34**(2): 267-273. doi: 10.1139/x03-183.

Keenan, T., Maria Serra, J., Lloret, F., Ninyerola, M., and Sabate, S. 2011. Predicting the future of forests in the Mediterranean under climate change, with niche- and process-based models: CO2 matters! Glob. Change Biol. **17**(1): 565-579. doi: 10.1111/j.1365-2486.2010.02254.x.

Key, T., Warner, T.A., McGraw, J.B., and Fajvan, M.A. 2001. A Comparison of Multispectral and Multitemporal Information in High Spatial Resolution Imagery for Classification of Individual Tree Species in a Temperate Hardwood Forest. Remote Sens. Environ. **75**(1): 100-112. doi: 10.1016/S0034-4257(00)00159-0.

Kornus, W., and Ruiz, A. 2003. Strip adjustment of LIDAR data. 3-D Reconstruction from Airborne Laserscanner and InSAR Data **34**(3): 47-50.

Kukko, A., Kaasalainen, S., and Litkey, P. 2008. Effect of incidence angle on laser scanner intensity and surface data. Appl. Opt. **47**(7): 986-992. doi: 10.1364/AO.47.000986.

Latifi, H., Fassnacht, F., and Koch, B. 2012. Forest structure modeling with combined airborne hyperspectral and LiDAR data. Remote Sens. Environ. **121**(0): 10-25. doi: 10.1016/j.rse.2012.01.015.

Leeuwen, W.J.D.v., Casady, G.M., Neary, D.G., Bautista, S., Alloza, J.A., Carmel, Y., Wittenberg, L., Malkinson, D., and Orr, B.J. 2010. Monitoring post-wildfire vegetation response with remotely sensed time-series data in Spain, USA and Israel. Int. J. Wildland Fire **19**(1): 75-93. doi: 10.1071/WF08078

Lefsky, M.A., Cohen, W.B., Parker, G.G., and Harding, D.J. 2002. Lidar remote sensing for ecosystem studies. Bioscience **52**(1): 19-30. doi: 10.1641/0006-3568

Liaw, A., and Wiener, M. 2002. Classification and Regression by randomForest. R News **2**(3): 18–22.

Lindner, M., Maroschek, M., Netherer, S., Kremer, A., Barbati, A., Garcia-Gonzalo, J., Seidl, R., Delzon, S., Corona, P., Kolstrom, M., Lexer, M.J., and Marchetti, M. 2010. Climate change impacts, adaptive capacity, and vulnerability of European forest ecosystems. Forest. Ecol. Manag. **259**(4): 698-709. doi: 10.1016/j.foreco.2009.09.023.

Loepfe, L., Martinez-Vilalta, J., Oliveres, J., Piñol, J., and Lloret, F. 2010. Feedbacks between fuel reduction and landscape homogenisation determine fire regimes in three Mediterranean areas. Forest. Ecol. Manag. **259**(12): 2366-2374. doi: 10.1016/j.foreco.2010.03.009.

Martin-Alcon, S., Coll, L., and Aunos, A. 2012. A broad-scale analysis of the main factors determining the current structure and understory composition of Catalonian sub-alpine (Pinus uncinata Ram.) forests. Forestry **85**(2): 225-236. doi: 10.1093/forestry/cpr067.

Martínez, L., Pérez, F., Arbiol, R., and Magariños, A. 2012. Development of NDVI WMS geoservice from reflectance DMC imagery at ICC. *In* International Calibration and Orientation Workshop EuroCOW 2012, Castelldefels (Barcelona).

McGaughey, R.J., and Carson, W.W. 2003. Fusing LIDAR data, photographs, and other data using 2D and 3D visualization techniques. *In* Terrain Data: Applications and Visualization – Making the Connection. *Edited by* A.S.f.P.a.R. Sensing, Charleston, South Carolina. pp. 16-24.

Morsdorf, F., Kötz, B., Meier, E., Itten, K.I., and Allgöwer, B. 2006. Estimation of LAI and fractional cover from small footprint airborne laser scanning data based on gap fraction. Remote Sens. Environ. **104**(1): 50-61. doi: 10.1016/j.rse.2006.04.019.

Moya, D., Heras, J.D.L., Lopez-Serrano, F.R., and Leone, V. 2008. Optimal intensity and age of management in young Aleppo pine stands for post-fire resilience. Forest. Ecol. Manag. **255**(8-9): 3270-3280. doi: 10.1016/j.foreco.2008.01.067.

Mutlu, M., Popescu, S.C., Stripling, C., and Spencer, T. 2008. Mapping surface fuel models using lidar and multispectral data fusion for fire behavior. Remote Sens. Environ. **112**(1): 274-285. doi: 10.1016/j.rse.2007.05.005.

Ordoñez, J.L., and Retana, J. 2004. Early reduction of post-fire recruitment of Pinus nigra by post-dispersal seed predation in different time-since-fire habitats. Ecography **27**(4): 449-458. doi: 10.1111/j.0906-7590.2004.03886.x.

Pausas, J.C., Llovet, J., Rodrigo, A., and Vallejo, R. 2008. Are wildfires a disaster in the Mediterranean basin? - A review. Int. J. Wildland Fire **17**(6): 713-723. doi: 10.1071/wf07151.

Pausas, J.G., Ribeiro, E., and Vallejo, R. 2004. Post-fire regeneration variability of Pinus halepensis in the eastern Iberian Peninsula. Forest. Ecol. Manag. **203**(1-3): 251-259. doi: 10.1016/j.foreco.2004.07.061.

Pierce, A.D., Farris, C.A., and Taylor, A.H. 2012. Use of random forests for modeling and mapping forest canopy fuels for fire behavior analysis in Lassen Volcanic National Park, California, USA. Forest. Ecol. Manag. **279**(0): 77-89. doi: 10.1016/j.foreco.2012.05.010.

Piñol, J., Terradas, J., and Lloret, F. 1998. Climate warming, wildfire hazard, and wildfire occurrence in coastal eastern Spain. Climatic Change **38**(3): 345-357.

Proença, V., Pereira, H.M., and Vicente, L. 2010. Resistance to wildfire and early regeneration in natural broadleaved forest and pine plantation. Acta Oecol. **36**(6): 626-633. doi: DOI: 10.1016/j.actao.2010.09.008.

Puerta-Piñero, C., Brotons, L., Coll, L., and González-Olabarría, J.R. 2011. Valuing acorn dispersal and resprouting capacity ecological functions to ensure Mediterranean forest resilience after fire. Eur. J. For. Res. **131**(3): 835-844. doi: 10.1007/s10342-011-0557-6.

Puerta-Piñero, C., Espelta, J.M., Sánchez-Humanes, B., Rodrigo, A., Coll, L., and Brotons, L. 2012. History matters: previous land use changes determine post-fire vegetation recovery in forested Mediterranean landscapes. Forest. Ecol. Manag. **279**: 121-127. doi: 10.1016/j.foreco.2012.05.020

R Development Core Team. 2007. R: A Language and Environment for Statistical Computing.

Rempel, R.S., Kaukinen., D., and Carr., A.P. 2012. Patch Analyst and Patch Grid. *Edited by* Ontario Ministry of Natural Resources. Centre for Northern Forest Ecosystem Research, Thunder Bay, Ontario.

Reque, J.A., and Bravo, F. 2008. Identifying forest structure types using National Forest Inventory Data: the case of sessile oak forest in the Cantabrian range. Inv. Agrar: Sist. Recursos Fores. **17**(2): 105-113.

Resco de Dios, V., Fischer, C., and Colinas, C. 2006. Climate Change Effects on Mediterranean Forests and Preventive Measures. New For. **33**(1): 29-40. doi: 10.1007/s11056-006-9011-x.

Retana, J., Arnan, X., Arianoutsou, M., Barbati, A., Kazanis, D., and Rodrigo, A. 2012. Post-Fire Management of Non-Serotinous Pine Forests. *In* Post-Fire Management and Restoration of Southern European Forests. *Edited by* F. Moreira and M. Arianoutsou and P. Corona and J. De las Heras. Springer Netherlands. pp. 151-170.

Retana, J., Espelta, J.M., Habrouk, A., Ordonez, J.L., and de Sola-Morales, F. 2002. Regeneration patterns of three Mediterranean pines and forest changes after a large wildfire in northeastern Spain. Ecoscience **9**(1): 89-97.

Riaño, D., Chuvieco, E., Ustin, S., Zomer, R., Dennison, P., Roberts, D., and Salas, J. 2002. Assessment of vegetation regeneration after fire through multitemporal analysis of AVIRIS images in the Santa Monica Mountains. Remote Sens. Environ. **79**(1): 60-71. doi: 10.1016/S0034-4257(01)00239-5.

Riaño, D., Chuvieco, E., Ustin, S.L., Salas, J., Rodríguez-Pérez, J.R., Ribeiro, L.M., Viegas, D.X., Moreno, J.M., and Fernández, H. 2007. Estimation of shrub height for fuel-type mapping combining airborne LiDAR and simultaneous color infrared ortho imaging. Int. J. Wildland Fire **16**(3): 341-348. doi: 10.1071/WF06003.

Rodrigo, A., Retana, J., and Picó, F.X. 2004. Direct regeneration is not the only response of Mediterranean forests to large fires. Ecology **85**(3): 716-729. doi: 10.1890/02-0492.

San-Miguel-Ayanz, J., Schulte, E., Schmuck, G., and Camia, A. 2013. The European Forest Fire Information System in the context of environmental policies of the European Union. Forest Policy and Economics **29**(0): 19-25. doi: 10.1016/j.forpol.2011.08.012.

Sanchez-Humanes, B., and Espelta, J.M. 2011. Increased drought reduces acorn production in Quercus ilex coppices: thinning mitigates this effect but only in the short term. Forestry **84**(1): 73-82. doi: 10.1093/forestry/cpq045.

Schelhaas, M.J., Nabuurs, G.J., and Schuck, A. 2003. Natural disturbances in the European forests in the 19th and 20th centuries. Glob. Change Biol. **9**(11): 1620-1633. doi: 10.1046/j.1365-2486.2003.00684.x

Selkimäki, M., González-Olabarria, J.R., and Pukkala, T. 2012. Site and stand characteristics related to surface erosion occurrence in forests of Catalonia (Spain). Eur. J. For. Res. **131** (3): 727-738. doi: 10.1007/s10342-011-0545-x

Shatford, J.P.A., Hibbs, D.E., and Puettmann, K.J. 2007. Conifer regeneration after forest fire in the Klamath-Siskiyous: How much, how soon? J. Forest. **105**(3): 139-146.

Stephens, S.L., Millar, C.I., and Collins, B.M. 2010. Operational approaches to managing forests of the future in Mediterranean regions within a context of changing climates. Environ. Res. Lett. **5**(2): 1-9. doi: 10.1088/1748-9326/5/2/024003.

Terrasolid. 2012. TerraScan User's Guide. Terrasolid, Helsinki.

Tucker, C.J. 1979. Red and photographic infrared linear combinations for monitoring vegetation. Remote Sens. Environ. **8**(2): 127-150. doi: 10.1016/0034-4257(79)90013-0.

Vallejo, V.R., Arianoutsou, M., and Moreira, F. 2012. Fire Ecology and Post-Fire Restoration Approaches in Southern European Forest Types. *In* Post-Fire Management and Restoration of Southern European Forests. *Edited by* F. Moreira and M. Arianoutsou and P. Corona and J. De las Heras. Springer Netherlands. pp. 93-119.

Verkaik, I., and Espelta, J.M. 2006. Post-fire regeneration thinning, cone production, serotiny and regeneration age in Pinus halepensis. Forest. Ecol. Manag. **231**(1–3): 155-163. doi: 10.1016/j.foreco.2006.05.041.

Vicente-Serrano, S.M., Pérez-Cabello, F., and Lasanta, T. 2011. Pinus halepensis regeneration after a wildfire in a semiarid environment: assessment using multitemporal Landsat images. Int. J. Wildland Fire **20**(2): 195-208. doi: 10.1071/WF08203.

Viedma, O., Meliá, J., Segarra, D., and Garcia-Haro, J. 1997. Modeling rates of ecosystem recovery after fires by using landsat TM data. Remote Sens. Environ. **61**(3): 383-398. doi: 10.1016/S0034-4257(97)00048-5.

Vilà-Cabrera, A., Rodrigo, A., Martínez-Vilalta, J., and Retana, J. 2012. Lack of regeneration and climatic vulnerability to fire of Scots pine may induce vegetation shifts at the southern edge of its distribution. J. Biogeogr. **39**(3): 488-496. doi: 10.1111/j.1365-2699.2011.02615.x.

Vila, J.P.S., and Barbosa, P. 2010. Post-fire vegetation regrowth detection in the Deiva Marina region (Liguria-Italy) using Landsat TM and ETM plus data. Ecol. Model. **221**(1): 75-84. doi: 10.1016/j.ecolmodel.2009.03.011.

Ward, J.H., Jr. . 1963. Hierarchical Grouping to Optimize an Objective Function. J. Am. Statist. Assoc.(58): 236–244.

Waser, L.T., Ginzler, C., Kuechler, M., Baltsavias, E., and Hurni, L. 2011. Semi-automatic classification of tree species in different forest ecosystems by spectral and geometric variables derived from Airborne Digital Sensor (ADS40) and RC30 data. Remote Sens. Environ. **115**(1): 76-85. doi: 10.1016/j.rse.2010.08.006.

Wulder, M.A., White, J.C., Alvarez, F., Han, T., Rogan, J., and Hawkes, B. 2009. Characterizing boreal forest wildfire with multi-temporal Landsat and LIDAR data. Remote Sens. Environ. **113**(7): 1540-1555. doi: 10.1016/j.rse.2009.03.004.

Wulder, M.A., White, J.C., Nelson, R.F., Næsset, E., Ørka, H.O., Coops, N.C., Hilker, T., Bater, C.W., and Gobakken, T. 2012. Lidar sampling for large-area forest characterization: A review. Remote Sens. Environ. **121**(0): 196-209. doi: 10.1016/j.rse.2012.02.001.

Tables

Table 1: Descriptive statistics (mean and standard deviation) of the main field variables (see abbreviations in section 2. 2. 3) for each of the regeneration types obtained in the 5-type classification generated by Ward's method clustering.

TYPE	n	%SOIL	%LOW SHRUBS	%HIGH SHRUBS	%TREES	%PINES	H_HW	H_PINES
1	5	54.11 (10.21)	39.11 (10.91)	3.21 (1.21)	3.61 (5.31)	0.41 (0.31)	84.31 (111.61)	55.91 (62.71)
2	5	28.71 (5.01)	39.91 (18.51)	24.41 (19.21)	7.01 (4.51)	1.91 (2.71)	125.61 (116.71)	130.91 (125.91)
3	11	26.61 (6.61)	28.41 (11.11)	10.11 (7.31)	34.91 (7.81)	7.71 (7.81)	272.41 (104.31)	122.61 (71.01)
4	10	14.81 (6.11)	17.41 (6.51)	14.71 (13.31)	53.11 (9.51)	6.61 (6.81)	361.61 (67.91)	119.81 (60.41)
5	13	13.71 (5.81)	20.91 (14.31)	8.51 (9.51)	57.01 (17.31)	45.41 (16.51)	215.51 (145.51)	206.11 (53.61)

Table 2: Basic patch size and shape characterization of the 5 regeneration types in the study area (PSm: patch size–mean; PScv: patch size–coefficient of variation; MSI: mean shape index)

TYPE	Area (ha)	Area (% of total)	% of TYPE area by size classes				PSm (ha)	PScv (%)	MSI
			< 0.1 ha	0.1-1 ha	1-5 ha	> 5 ha			
1	298.3	9.35	79.16	20.84	0.00	0.00	0.0164	81.8	1.198
2	652.0	20.43	57.67	28.13	12.17	2.03	0.0177	83.1	1.232
3	532.3	16.68	80.26	19.55	0.20	0.00	0.0169	82.1	1.203
4	1359.0	42.58	32.63	36.32	25.15	5.90	0.0198	86.1	1.291
5	350.2	10.97	59.96	30.04	7.76	2.23	0.0177	85.0	1.223
TOTAL	3191.8								

Figures

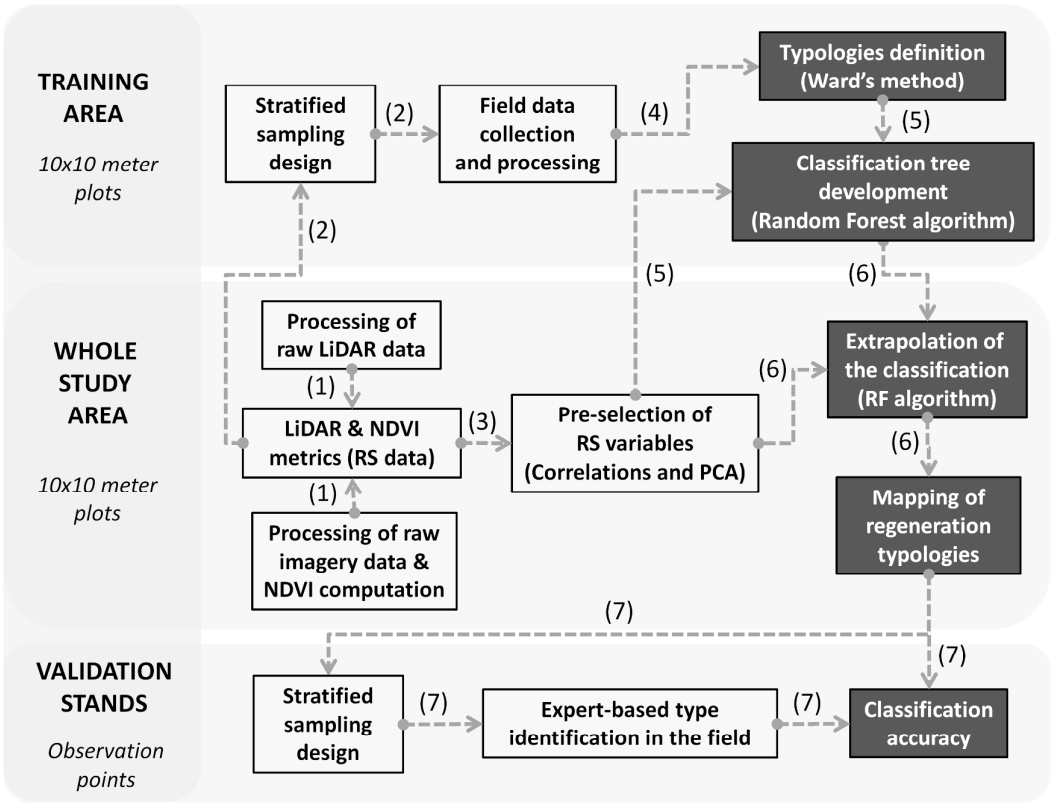

Figure 1: Flowchart schematizing the methodological approach. Numbers indicate the step order.

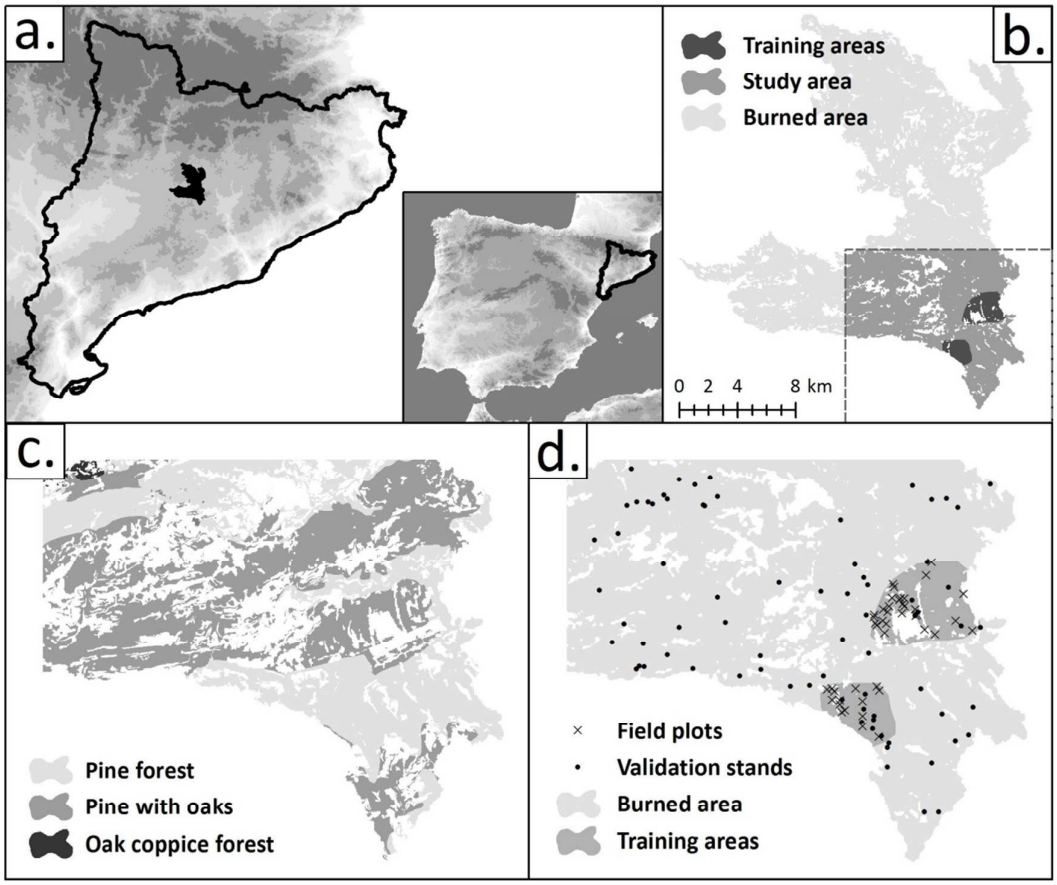

Figure 2: Location and boundaries of: a) the wildfire location in the Iberian Peninsula and Catalonia region; b) the study area and the calibration areas within the wildfire zone; c) the dominant forest types in the study area before the 1998 wildfire (CREAF 1993; DGCN 2001); d) the field plots and the validation stands within the study area.

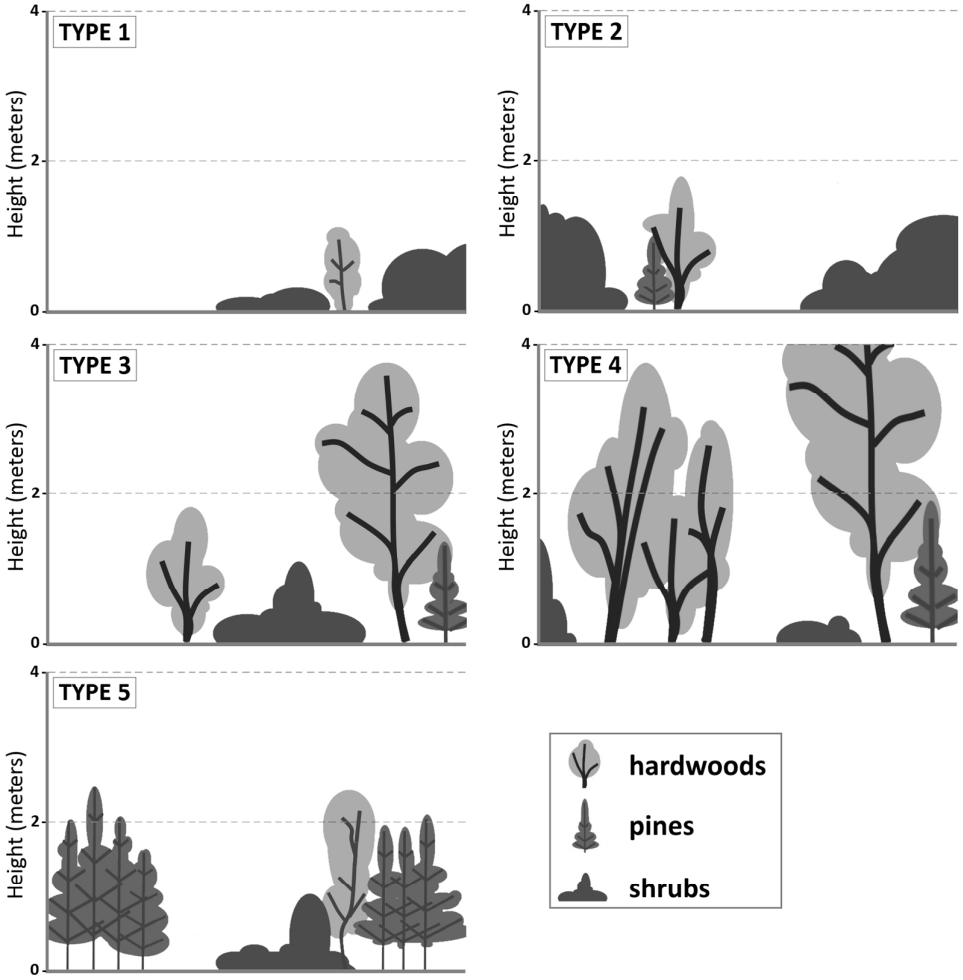

Figure 3: Schematic interpretation of the 56 post-fire regeneration types obtained from Ward's method clustering. Regeneration types are: TYPE 1 (defective cover of woody vegetation), TYPE 2 (dominance of shrubs cover), TYPE 3 (hardwoods low-moderate cover), TYPE 4 (hardwoods high cover), TYPE 5 (pines moderate-high cover).

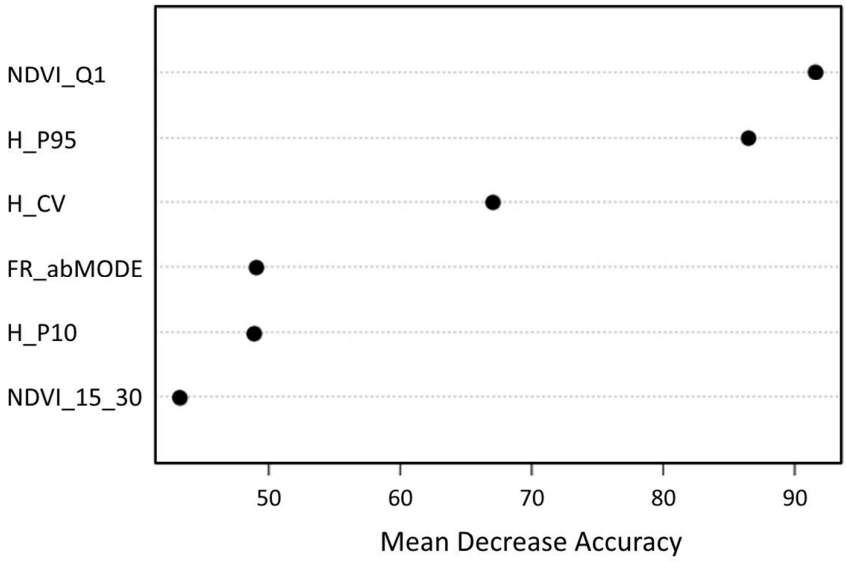

Figure 4: Variable importance plots for the for the 5-type classification model of post-fire regeneration types. Higher value of Mean Decrease Accuracy represents higher variable importance in the model.

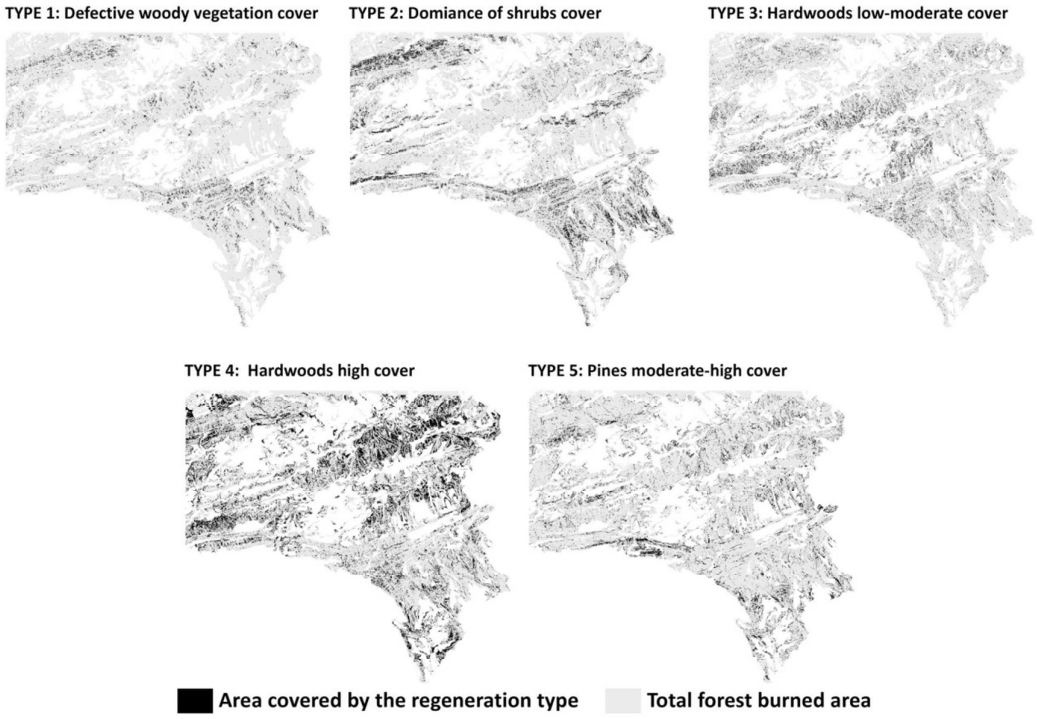

Figure 5: Spatial distribution of regeneration types in the study area. In black, the area covered by each of the regeneration typologies.

Supplementary material

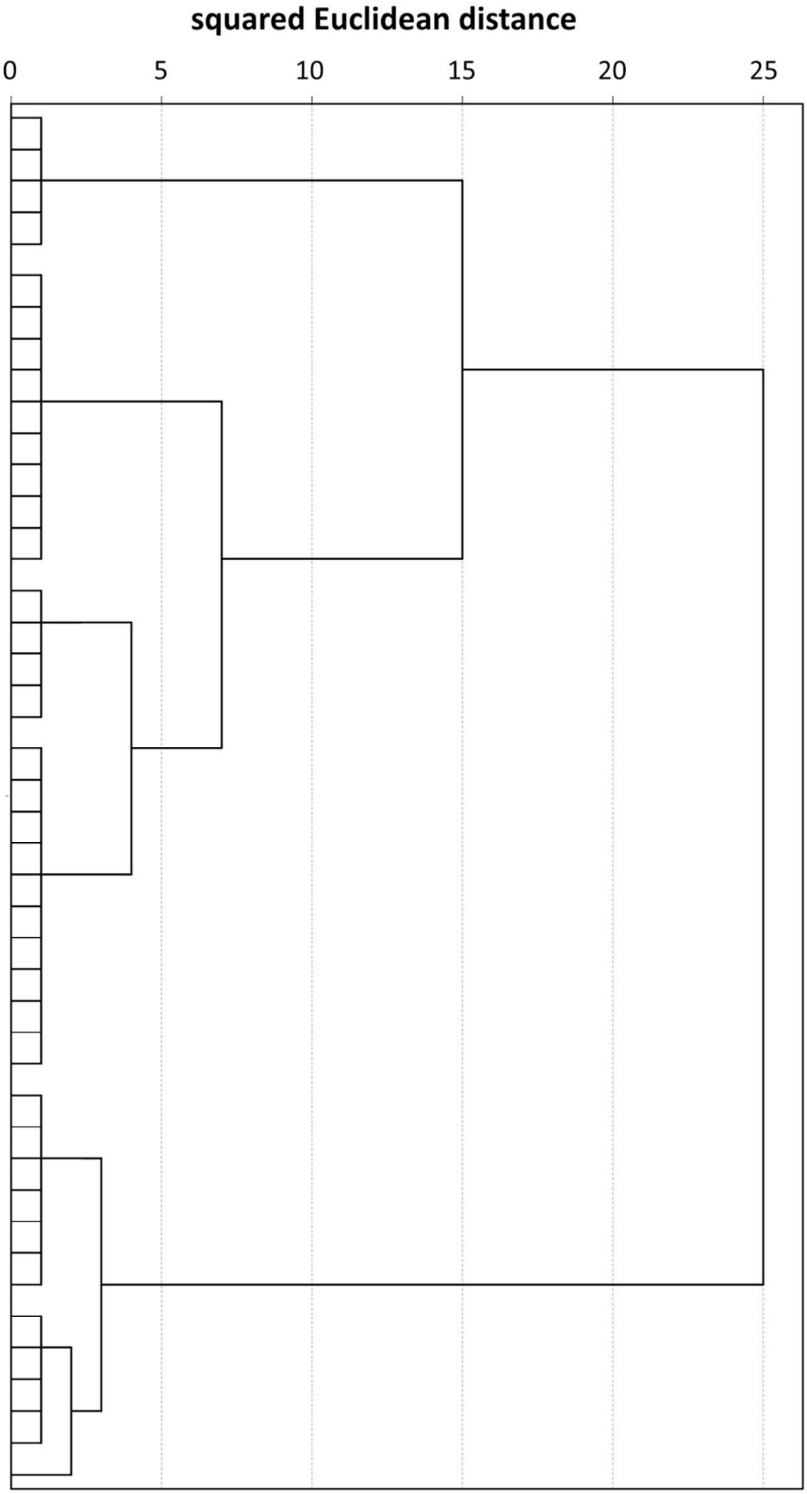

Figure 1S: Dendrogram illustrating the result of the cluster analysis using Ward's method applied on forest variables measured in the field plots (n = 44)

Table 1S: Descriptive statistics (mean and standard deviation) of the main field variables (see abbreviations in section 2. 2. 3) for each of the regeneration types obtained in the 4-type classification after Ward's method clustering.

TYPE	n	%SOIL	%LOW SHRUBS	%HIGH SHRUBS	%TREES	%PINES	H_HW	H_PINES
1	5	54.11 (10.21)	39.11 (10.91)	3.21 (1.21)	3.61 (5.31)	0.41 (0.31)	84.31 (111.61)	55.91 (62.71)
2	16	27.31 (6.01)	32.01 (14.31)	14.61 (13.51)	26.21 (15.01)	5.91 (7.11)	226.51 (125.81)	125.21 (87.21)
3	10	14.81 (6.11)	17.41 (6.51)	14.71 (13.31)	53.11 (9.51)	6.61 (6.81)	361.61 (67.91)	119.81 (60.41)
4	13	13.71 (5.81)	20.91 (14.31)	8.51 (9.51)	57.01 (17.31)	45.41 (16.51)	215.51 (145.51)	206.11 (53.61)

Table 2S: Descriptive statistics (mean and standard deviation) of the main field variables (see abbreviations in section 2. 2. 3) for each of the regeneration types obtained in the 6-type classification after Ward's method clustering.

TYPE	n	%SOIL	%LOW SHRUBS	%HIGH SHRUBS	%TREES	%PINES	H_HW	H_PINES
1	5	54.11 (10.21)	39.11 (10.91)	3.21 (1.21)	3.61 (5.31)	0.41 (0.31)	84.31 (111.61)	55.91 (62.71)
2	5	28.71 (5.01)	39.91 (18.51)	24.41 (19.21)	7.01 (4.51)	1.91 (2.71)	125.61 (116.71)	130.91 (125.91)
3	11	26.61 (6.61)	28.41 (11.11)	10.11 (7.31)	34.91 (7.81)	7.71 (7.81)	272.41 (104.31)	122.61 (71.01)
4	10	14.81 (6.11)	17.41 (6.51)	14.71 (13.31)	53.11 (9.51)	6.61 (6.81)	361.61 (67.91)	119.81 (60.41)
5	7	16.81 (6.11)	27.71 (15.51)	12.01 (11.71)	43.51 (7.31)	36.81 (10.11)	166.51 (129.91)	200.91 (48.11)
6	6	10.11 (2.91)	12.91 (7.91)	4.41 (3.81)	72.71 (10.31)	55.41 (17.41)	272.81 (152.41)	212.11 (63.51)

Table 1: Descriptive statistics (mean and standard deviation) of the main field variables (see abbreviations in section 2. 2. 3) for each of the regeneration types obtained in the 5-type classification generated by Ward's method clustering.

TYPE	n	%SOIL	%LOW SHRUBS	%HIGH SHRUBS	%TREES	%PINES	H_HW	H_PINES
1	5	54.11 (10.21)	39.11 (10.91)	3.21 (1.21)	3.61 (5.31)	0.41 (0.31)	84.31 (111.61)	55.91 (62.71)
2	5	28.71 (5.01)	39.91 (18.51)	24.41 (19.21)	7.01 (4.51)	1.91 (2.71)	125.61 (116.71)	130.91 (125.91)
3	11	26.61 (6.61)	28.41 (11.11)	10.11 (7.31)	34.91 (7.81)	7.71 (7.81)	272.41 (104.31)	122.61 (71.01)
4	10	14.81 (6.11)	17.41 (6.51)	14.71 (13.31)	53.11 (9.51)	6.61 (6.81)	361.61 (67.91)	119.81 (60.41)
5	13	13.71 (5.81)	20.91 (14.31)	8.51 (9.51)	57.01 (17.31)	45.41 (16.51)	215.51 (145.51)	206.11 (53.61)

Table 2: Basic patch size and shape characterization of the 5 regeneration types in the study area (PSm: patch size–mean; PScv: patch size–coefficient of variation; MSI: mean shape index)

TYPE	Area (ha)	Area (% of total)	% of TYPE area by size classes				PSm (ha)	PScv (%)	MSI
			< 0.1 ha	0.1-1 ha	1-5 ha	> 5 ha			
1	298.3	9.35	79.16	20.84	0.00	0.00	0.0164	81.8	1.198
2	652.0	20.43	57.67	28.13	12.17	2.03	0.0177	83.1	1.232
3	532.3	16.68	80.26	19.55	0.20	0.00	0.0169	82.1	1.203
4	1359.0	42.58	32.63	36.32	25.15	5.90	0.0198	86.1	1.291
5	350.2	10.97	59.96	30.04	7.76	2.23	0.0177	85.0	1.223
TOTAL	3191.8								